Prospects of Searches for Neutral, Long-Lived Particles which Decay to Photons using Timing at CDF

David Toback* and Peter Wagner†

Texas A&M University, College Station, Texas 77843-4242

We present the prospects of searches for neutral, long-lived particles which decay to photons using their time of arrival measured with a newly installed timing system on the electromagnetic calorimeter (EMTiming) of the Collider Detector at Fermilab (CDF). A Monte Carlo simulation shows that EMTiming can provide separation between decay photons from particles with both a long lifetime and a low boost, and prompt photons from Standard Model backgrounds. Using a gauge mediated supersymmetry breaking (GMSB) $\tilde{\chi}_1^0 \to \gamma \tilde{G}$ model we estimate a quasi-model-independent sensitivity using only direct neutralino pair production, and also estimate the expected 95% confidence level exclusion regions for all superpartner production as a function of the neutralino mass and lifetime. We find that a combination of single photon and diphoton analyses should allow the Tevatron in run II to easily extend the exclusion regions from LEP II at high neutralino masses and lifetimes, and cover much, if not all, of the theoretically favored $m_{\tilde{G}} < 1$ keV/c^2 parameter space for neutralino masses less than 150 GeV/c^2.

I. INTRODUCTION

The electromagnetic (EM) calorimeter at the Collider Detector at Fermilab (CDF) [1] has recently been equipped with a new nanosecond-resolution timing system, EMTiming [2], to measure the arrival time of energy deposited (e.g. from photons). While it was initially designed to reject cosmics and accelerator backgrounds [3], we investigate the possibility of using it to search for neutral particles [4] with a lifetime of the order of a nanosecond which decay in flight to photons. An example of a theory which would produce these particles is the gauge mediated supersymmetry breaking (GMSB) model [5] with a neutralino, $\tilde{\chi}_1^0$, as the next-to-lightest supersymmetric particle (NLSP) and a light gravitino, $\tilde{G}$, as the LSP. In this scenario the neutralino decays preferably ($\sim$100%) as $\tilde{\chi}_1^0 \to \gamma \tilde{G}$ with a macroscopic lifetime for much of the GMSB parameter space.

We begin with a study of the properties of events where timing can be used to separate between decay photons from long-lived particles, and photons produced promptly at the collision. A suitable variable to describe this distinction is the measured difference between the time after which the photon arrives at the face of the detector, and the time a prompt photon would virtually need to reach the same final position. This time difference for a prompt photon, from Standard Model (SM) sources, is exactly 0 but is always greater than 0 for photons from delayed decays, as in GMSB/Supersymmetry, if we neglect the measurement resolution. We call this difference Δs:

$$\Delta s \equiv (t_f - t_i) - \frac{|\vec{x}_f - \vec{x}_i|}{c} \qquad (1)$$

where $t_f - t_i$ is the time between the collision and the arrival time of the photon at the face of the detector, and $|\vec{x}_f - \vec{x}_i|$ is the distance between the final position of the photon and the collision point. The situation is visualized in Fig. 1. All four variables can be measured by the CDF detector [6] and give a system resolution of $\sigma_{\text{EMTiming}} \sim 1.0$ ns [7].

An important note in our analysis is that photons from long-lived particles will usually not arrive at the face of the EM calorimeter at the usual 90 degree incident angle. This could have serious implications for photon identification. For the purposes of this study we assume that this issue can be addressed without significant changes to the identification efficiency. We further assume that the additional handles such as EMTiming and timing in the hadronic calorimeters provide the necessary robustness needed to convince ourselves that photons which might not pass ordinary selection requirements are indeed from our signal source as opposed to sources which could produce fake photons and missing transverse energy, $\not{E}_T$, like cosmics.

We estimate our sensitivity to two different types of new particle production using GMSB models. As a quasi-model-independent sensitivity estimate to generic long-lived particles we simulate direct neutralino pair production and decay, and examine the dependency as a function of both neutralino mass, $m_{\tilde{\chi}}$, and lifetime, $\tau_{\tilde{\chi}}$. For a "full" GMSB model sensitivity, which means including all relevant GMSB subprocesses such that the neutralinos are part of cascades from gauginos and squarks, we allow all SUSY particle production and decay, and again vary the mass and lifetime variables. To choose analysis final states for both we consider three issues: 1) with neutralino lifetimes longer than a nanosecond it is possible that one or both of the neutralinos leave the detector before they decay, 2) with gravitinos or the neutralino leaving the detector $\not{E}_T$ should also help separate signal from SM backgrounds and 3) to ensure that our predictions are as reliable as possible we want to use the data
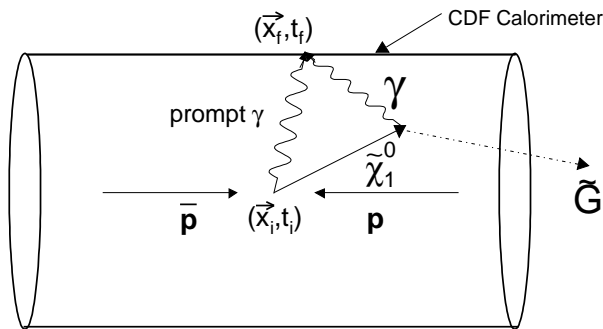
Figure 1: A schematic diagram of a long-lived neutralino decaying to a photon and a gravitino in the CDF detector. The neutralino emanates from the collision at $(\vec{x}_i, t_i)$ and after a time τ it decays. While the gravitino leaves the detector the photon travels to the detector wall and deposits energy in the EM calorimeter where its final location $\vec{x}_f$ and arrival time t_f can be measured. A prompt photon would travel directly from $\vec{x}_i$ to $\vec{x}_f$ which can both be measured. The difference between the actual time the neutralino/photon needs, $\Delta t = t_f - t_i$, and the time a prompt photon would need, $\frac{|\vec{x}_f - \vec{x}_i|}{c}$, is defined as Δs. The SM typically produces prompt photons which have $\Delta s = 0$ ns, whereas photons from delayed decays from SUSY have $\Delta s > 0$ ns, assuming a perfect measurement.

selection requirements and background predictions from previously published papers by CDF [1] and DØ [8]. In the 1992-1995 collider run (run I) of the Tevatron three types of analyses match these criteria: CDF and DØ results in $\gamma\gamma + \not{E}_T$ [3, 9], exclusive $\gamma + \not{E}_T$ ($\gamma + \not{E}_T + 0$ jets) from CDF [10] and $\gamma + \not{E}_T +$ jets from DØ [11]. Since there are no jets at the parton level in direct neutralino pair production, in this case we consider analyses with final states $\gamma\gamma + \not{E}_T$ and $\gamma + \not{E}_T + 0$ jets. To estimate the sensitivity for full GMSB neutralino production we consider both $\gamma\gamma + \not{E}_T$ and $\gamma + \not{E}_T +$ jets analyses.

For both direct neutralino pair production and full GMSB production we quantify the sensitivity for 2 fb^{-1} in run II using the expected 95% confidence level (C.L.) cross section upper limits. Results for both with and without the EMTiming system, using kinematics cuts only, illustrate the contribution to the final sensitivity from kinematic and timing information considerations [12]. Finally, we compare the final mass and lifetime exclusion regions for a GMSB scenario to direct and indirect searches from the ALEPH experiment [13] at LEP II and the theoretically favored parameter space from cosmological model restrictions of $m_{\tilde{G}} < 1$ keV/c^2 [14].

II. KINEMATIC PROPERTIES OF EVENTS WITH LONG-LIVED PARTICLES WHICH DECAY TO PHOTONS

While the final sensitivity studies use both a full physics generation and a detector simulation of the geometry and timing resolution, we begin with a study of the kinematic properties of events which yield large Δs measurements using a "toy Monte Carlo." For now the CDF detector is assumed to be a cylinder, with length 3.5 m and radius 1.7 m, instrumented with time and position detectors of perfect resolution for both the collision point and where the photon hits the face of the detector. Neutral particles, which we will refer to as neutralinos, are simulated as emanating isotropically from the center of the detector and emit a photon isotropically after a lifetime $\tau_{\tilde{\chi}}$ in their rest frame. For a promptly decaying photon the minimum time corresponds to the nearest distance to the detector face: $\frac{1.7\text{m}}{c} = 5.6$ ns; the maximum to the largest distance $\sqrt{(1.7\text{m})^2 + (\frac{3.5\text{m}}{2})^2}/c = 8.1$ ns. For pedagogic reasons, neutralinos are simulated with a flat momentum and lifetime distribution, i.e. independently any lifetime and momentum have equal probability. We note that to be conservative here, as later in the paper, only those neutralinos that decay before the face of the detector are considered to have produced a photon.

Figure 2 shows the measured Δs versus the event lifetime of the $\tilde{\chi}_1^0$ in the lab frame, $\tau_{\text{evt,L}}$. For $\Delta s \gtrsim 10$ ns there is a roughly linear relation between Δs and $\tau_{\text{evt,L}}$. For a fixed $\tau_{\text{evt,L}}$ the maximum Δs (upper bound) occurs when the neutralino travels to the farthest corner of the detector and then emits a photon backward to the opposite corner. Analogously we get a minimum Δs (lower bound) if the neutralino travels with high momentum to the nearest part of the detector and emits a photon forward. The latter would look like a usual prompt photon event except for the difference in velocity between the neutralino and the photon. If the event lifetime is greater than the maximum time a prompt photon would need to travel to the detector then Δs is restricted from below and $\Delta s > 0$ ns (given that the neutralino decays inside the detector). Thus, the spread mainly comes from detector geometry but with the neutralino momentum also contributing to the width.

Figure 3 shows Δs versus the neutralino boost for the lifetime slice 8.5 ns $\leq \tau_{\text{evt,L}} \leq 9.0$ ns. A low boost (between 1.0 and 1.5) allows large Δs since neutralinos can have a larger lifetime without leaving the detector. Neutralinos with high boost are more likely to leave the detector, and even if they do not and their photon is detected, it has low Δs (0 ns $\lesssim \Delta s \lesssim 2$ ns). Thus, events with large Δs are produced by neutralinos with long lifetimes and low boost.

Next we consider the efficiency for neutralinos to remain in the detector and/or produce a photon with large Δs. Figure 4 shows the efficiency, the fraction of all generated events that produce photons which pass a given
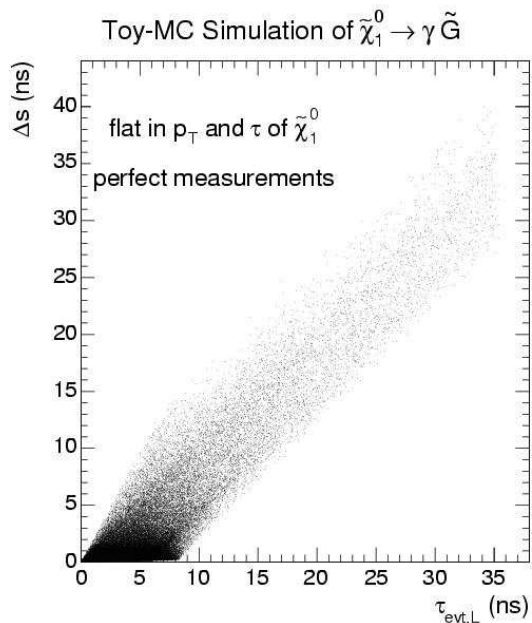
Toy-MC Simulation of $\tilde{\chi}_1^0 \to \gamma\tilde{G}$

flat in p_T and τ of $\tilde{\chi}_1^0$

perfect measurements

Toy-MC Simulation of $\tilde{\chi}_1^0 \to \gamma\tilde{G}$

flat in p_T and τ of $\tilde{\chi}_1^0$

perfect measurements

Figure 2: The Δs distribution as a function of the event lifetime in the neutralino lab frame for a toy Monte Carlo simulation. In general, Δs is proportional to $\tau_{\mathrm{evt,L}}$. At large $\tau_{\mathrm{evt,L}}$ most of the neutralinos leave the detector and are not shown here. The spread perpendicular to $\Delta s \sim \tau_{\mathrm{evt,L}}$ originates in variations of the neutralino momentum as well as in variations in the travel time of the photon due to detector geometry. Essentially, events with large Δs require a neutralino with a long lifetime.

Figure 3: The Δs distribution as a function of the boost of the neutralino for a lifetime "slice" of 8.5 ns $\leq \tau_{\mathrm{evt,L}} \leq$ 9.0 ns. In the region $1.0 <$ boost < 1.5 neutralinos remain in the detector and can produce a large Δs. Neutralinos with high boost, that is high p_T, are more likely to leave the detector or, if they don't, produce low Δs. Thus, events with the largest Δs are produced by neutralinos with large lifetimes and low boosts.

III. NEUTRALINO PAIR PRODUCTION AS A MEASURE OF QUASI-MODEL-INDEPENDENT SENSITIVITY

A. Analysis Methods and their Efficiency as a Function of Neutralino Mass and Lifetime

Δs restriction, as a function of the event lifetime, τ_{evt}, for $\Delta s \geq 0$ (neutralino stays in the detector), 3 ns and 5 ns for the same production distribution. While these results change for a more realistic p_T spectrum, the qualitative features are instructive. In the limit of $\tau_{\mathrm{evt}} = 0$ ns and $\Delta s \geq 0$ the efficiency is 100% and the efficiency decreases with higher event lifetime, since the neutralinos are more likely to leave the detector. When one applies a Δs cut however, there is no efficiency for events that contain neutralinos with a low event lifetime ($\tau_{\mathrm{evt}} \lesssim 2$ ns). For any $\Delta s > 0$ requirement the efficiency goes to 0% at $\tau_{\mathrm{evt}} = 0$ ns, since all photons would have $\Delta s = 0$. A higher Δs cut gradually suppresses events with a neutralino lifetime of about $\tau_{\mathrm{evt}} \lesssim 2 \cdot \Delta s$, whereas it does not suppress any events with a high lifetime. So, if an event contains a neutralino with a long lifetime and which decays in the detector, the decay photon always has high Δs.
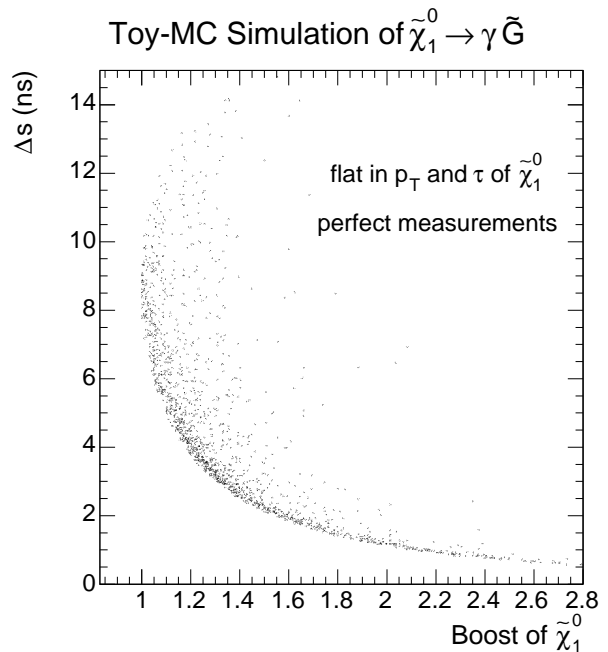
Here we estimate our sensitivity to neutral, long-lived particles which decay to photons in as model-independent a manner as possible. We do so by considering a GMSB model [15] which we restrict to direct neutralino pair production and decay: $p\bar{p} \to \tilde{\chi}_1^0 \tilde{\chi}_1^0 \to \gamma\tilde{G}\gamma\tilde{G}$. We use the PYTHIA [16] event generator, with ISAJET [17] to generate the SUSY masses, and PGS with the parameter file for the CDF detector [18] as a simple detector simulation, modified for the use of timing information. We accept photons with a rapidity $|\eta| \leq 2.1$ and a transverse energy $E_T \geq 12$ GeV according to the CDF/EMTiming fiducial region and trigger [1, 2]. We first look at the efficiency of the timing system with infinite resolution as a function of neutralino mass and lifetime for different Δs restrictions. Then we discuss background estimations, take into account a timing resolution of 1.0 ns and find the sensitivities for the model predictions for both the single and diphoton analysis.

Figure 5 shows the efficiency versus neutralino lifetime for a mass of 70 GeV/c^2 [19] for events with $\Delta s \geq 0$ ns (photons from neutralinos remaining in the detector) and events

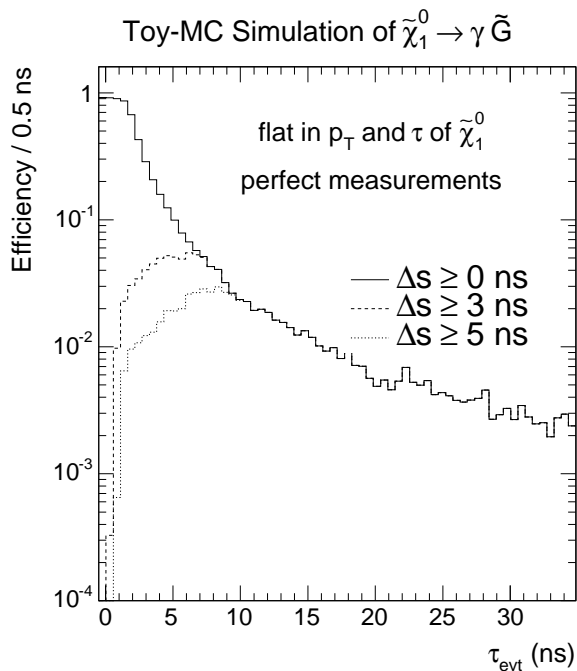## Toy-MC Simulation of $\widetilde{\chi}_1^0 \to \gamma \widetilde{G}$

flat in p_T and τ of $\widetilde{\chi}_1^0$

perfect measurements

$\Delta s \geq 0$ ns
$\Delta s \geq 3$ ns
$\Delta s \geq 5$ ns

Figure 4: The efficiency as a function of the event lifetime, τ_{evt}, of the neutralino. We distinguish between events in which the neutralino remains in the detector, and events with photons of medium and large Δs. The efficiency is 100% for prompt decays (a small difference shows up as a binning effect) for a photon to be identified, but only a very small efficiency for events with low τ_{evt} at large Δs. At large τ_{evt} only few events stay in the detector, however if a neutralino is long-lived and stays in the detector, it has large Δs. We note that the true efficiency shape depends on the production mechanism i.e. the neutralino p_T distribution.

with a $\Delta s \geq 5$ ns, separated into single and diphoton events. We get essentially the same shapes as in Fig. 4, however the overall efficiency is less as we now consider the exponentially distributed neutralino lifetime instead of an event lifetime. For all four distributions there is an efficiency maximum in the lifetime region between 4 and 9 ns. At lower lifetimes the probability that the neutralino stays in the detector is large enough that the diphoton final state dominates. For any $\Delta s > 0$ requirement the efficiency is zero at $\tau_{\widetilde{\chi}} = 0$ ns, since all photons have $\Delta s = 0$. At a lifetime of about 3 ns, independent of the Δs cut, single photon events become dominant. At high lifetimes the efficiency decreases rapidly for both analyses as most of the neutralinos leave the detector. Hence, in order to have sensitivity in as much lifetime range as possible, we consider both $\gamma + \not{E}_T$ and $\gamma\gamma + \not{E}_T$ analyses.

In contrast the timing efficiency is essentially constant as a function of neutralino mass at a fixed lifetime. Figure 6 shows the efficiencies at $\tau_{\widetilde{\chi}} = 10$ ns, where the system has the highest efficiency and single photon events dominate. Note that the "dip" in the efficiency can be explained by the neutralino pair production mechanism: if the decay length is greater than the distance to the detector wall, the neutralino will leave. Since this is proportional to the ratio of the neutralino's transverse momentum to its mass, $\frac{p_T}{m}$, (at constant lifetime), the dip

Table I: The systematic uncertainties, estimated based on Refs. [3, 11], for luminosity, acceptance and number of background events for use in all analyses in estimating cross section limits.

Factor	Syst. Uncertainty
Luminosity	5%
Acceptance	10%
Number of background events	30%

occurs from a change in the shape of the $\frac{p_T}{m}$ distribution of the neutralinos as shown in Fig. 7. For a mass of 80 GeV/c^2 the maximum moves towards higher $\frac{p_T}{m}$ and the distribution broadens compared to 40 GeV/c^2, yielding a greater fraction of high-p_T neutralinos and hence a loss in efficiency. As the mass gets higher the maximum remains the same and the distribution narrows, which in turn leads to a gain in efficiency. Thus, the efficiency is essentially independent of the neutralino mass, with slight variations originating from the production mechanism, specifically the neutralino momentum distribution.

B. Backgrounds and Sensitivity to Neutralino Pair Production

We now estimate the sensitivity of our system in a quasi-model-independent manner using the neutralino pair production introduced in the previous section, but taking into account SM backgrounds, more realistic cuts and the timing resolution. We consider separately single photon and diphoton events and present our sensitivity as the expected 95% C.L. cross section upper limits for either case assuming no signal in the data. We also compare our results with the results of no EMTiming system available to estimate the effect of the EMTiming system over a set of kinematics-only selection requirements. Throughout this section we use the relative systematic uncertainties for luminosity, acceptance and background rates given in Table I and a Δs resolution of 1.0 ns. The expected cross section limits are calculated following [20] with the number of events observed "in the data" fluctuating around an expected mean background rate according to Poisson statistics. The cross section limit is, for a certain luminosity, a function of background events and signal acceptance, where both in turn are functions of specified cuts (e.g. Δs and $\not{E}_T$ cuts in the $\gamma\gamma + \not{E}_T$ case). By varying the cuts we find a signal acceptance and number of background events that, after smearing by systematic errors, minimizes the cross section limit.

1. $\gamma\gamma + \not{E}_T$

A $\gamma\gamma + \not{E}_T$ analysis is expected to have the best sensitivity for low neutralino lifetimes. We follow the analysis in [3] (summarized in Table II) and allow events in which both photons have $E_T > 12$ GeV and $|\eta| < 1$, and study final selection requirements on $\not{E}_T$ and Δs. The background for this analysis consists of QCD events with fake $\not{E}_T$ [21]. We model the
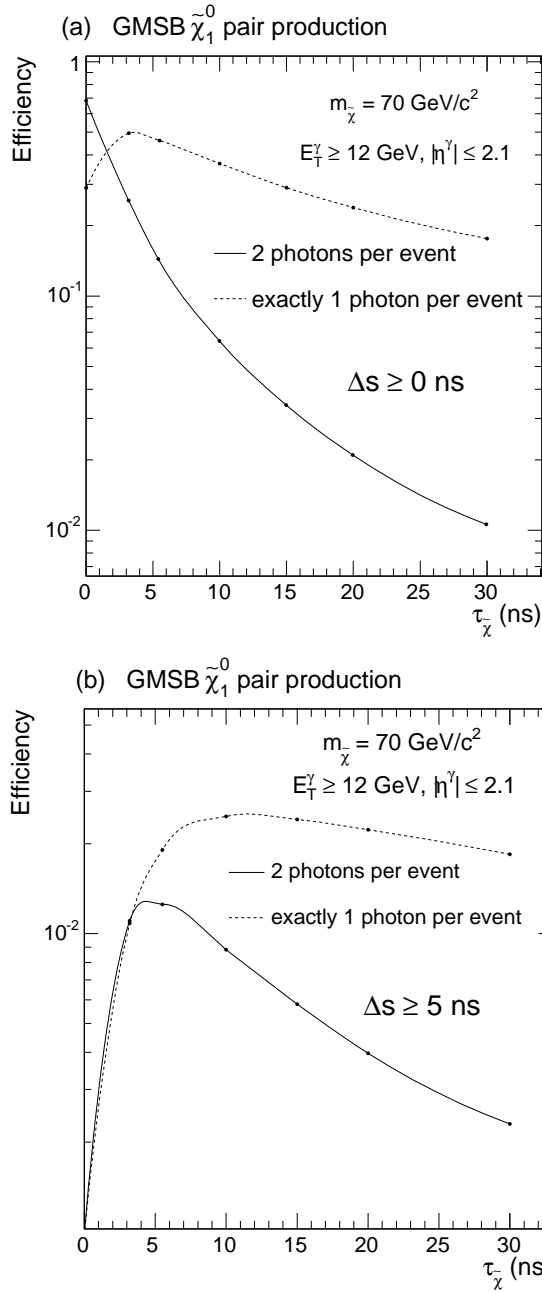
(a) GMSB $\tilde{\chi}^0_1$ pair production

$m_{\tilde{\chi}} = 70$ GeV/c^2

$E^\gamma_T \geq 12$ GeV, $|\eta^\gamma| \leq 2.1$

—— 2 photons per event

······ exactly 1 photon per event

$\Delta s \geq 0$ ns

(a) GMSB $\tilde{\chi}^0_1$ pair production

$\tau_\chi = 10$ ns

$E^\gamma_T \geq 12$ GeV, $|\eta^\gamma| \leq 2.1$

—— 2 photons per event

······ exactly 1 photon per event

$\Delta s \geq 0$ ns

(b) GMSB $\tilde{\chi}^0_1$ pair production

$m_{\tilde{\chi}} = 70$ GeV/c^2

$E^\gamma_T \geq 12$ GeV, $|\eta^\gamma| \leq 2.1$

—— 2 photons per event

······ exactly 1 photon per event

$\Delta s \geq 5$ ns

(b) GMSB $\tilde{\chi}^0_1$ pair production

$\tau_{\tilde{\chi}} = 10$ ns

$E^\gamma_T \geq 12$ GeV, $|\eta^\gamma| \leq 2.1$

—— 2 photons per event

······ exactly 1 photon per event

$\Delta s \geq 5$ ns

Figure 5: The efficiency for events to pass the various Δs-cuts (assuming perfect measurements) as a function of the neutralino lifetime at constant mass ($m_{\tilde{\chi}} = 70$ GeV/c^2), separated into single and diphoton events at $\Delta s \geq 0$ ns and 5 ns. For any $\Delta s > 0$ the efficiency is zero at $\tau_{\tilde{\chi}} = 0$ ns, since all photons would have $\Delta s = 0$. For high τ neutralinos have a higher probability to leave the detector. For any Δs one can find an efficiency maximum at about 5-10 ns. Single photon events are preferred towards higher Δs requirements and/or higher lifetimes, due to increasing probability for a photon to leave the detector. Thus, we expect a $\gamma\gamma + \not{E}_T$ to provide the best sensitivity for very low lifetimes, and a $\gamma + \not{E}_T$ analysis to be best for higher lifetimes.
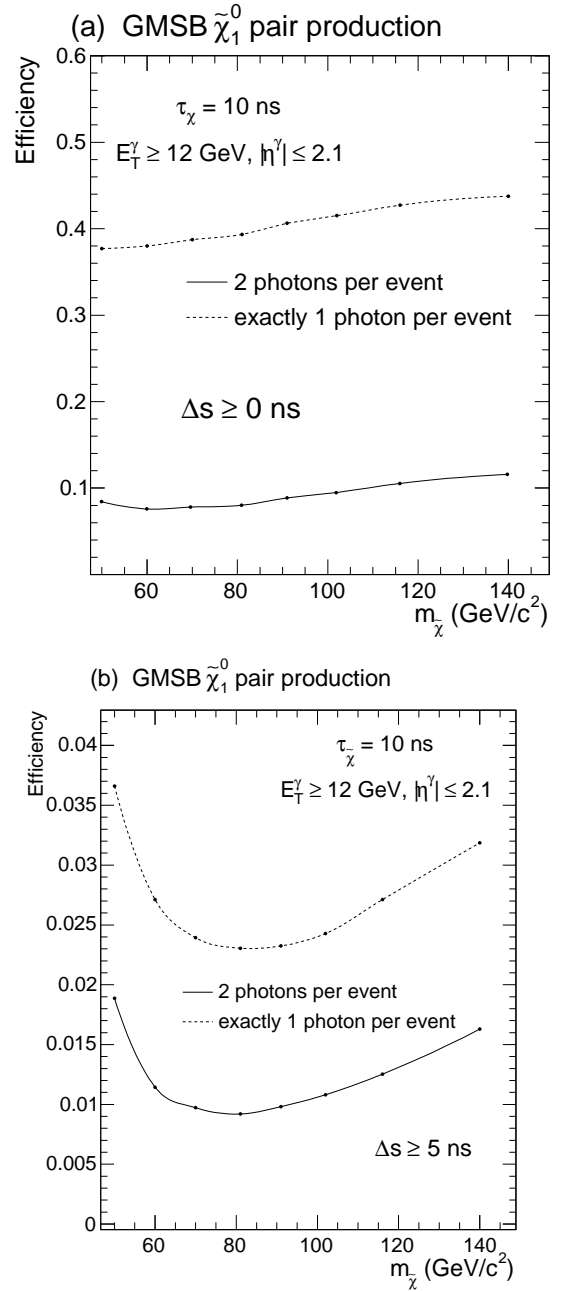
Figure 6: The efficiency as a function of the neutralino mass at a lifetime $\tau_{\tilde{\chi}} = 10$ ns for single and diphoton events at $\Delta s \geq 0$ ns and 5 ns (assuming perfect measurements). The ratio of single to diphoton events is independent of the neutralino mass and is roughly constant as a function of Δs. One can see a soft "dip" in the efficiency curve in a mass range of 40 GeV/c^2−80 GeV/c^2. This effect is production dependent and due to a change in the p_T distribution of the neutralinos (see Fig. 7).
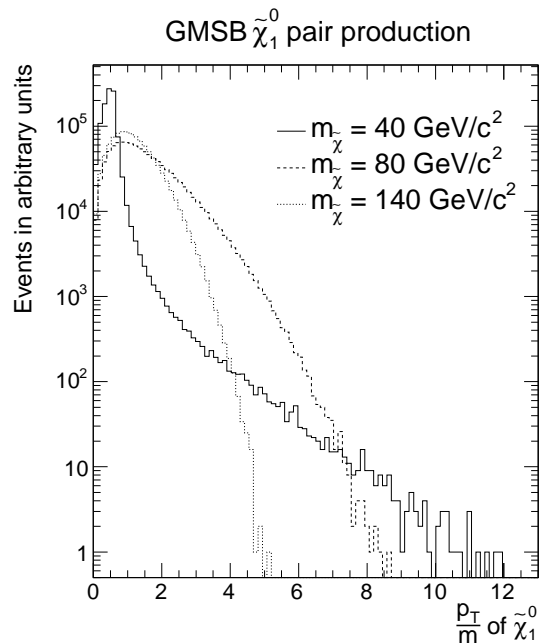
Figure 7: The neutralino $\frac{p_T}{m}$ distribution for masses 40 GeV/c^2, 80 GeV/c^2 and 140 GeV/c^2 for neutralino pair production. For a mass of 80 GeV/c^2 the maximum moves towards higher $\frac{p_T}{m}$ and the distribution broadens compared to 40 GeV/c^2, yielding a greater fraction of high p_T neutralinos which either leave the detector or produce low Δs photons, and thus a loss in efficiency. For higher masses the maximum remains constant and the distribution narrows so the efficiency rises.

$E\!\!\!/_T$ from QCD with a resolution of 10 GeV, i.e. we assume a measurement uncertainty of the transverse energy of all particles of 10 GeV in each x- and y-direction, as this reproduces well the numbers in [3] and allows us to extend our search region to large values of $E\!\!\!/_T$. Since all photons from QCD are promptly produced, we model them with a mean Δs of 0 ns, and a resolution of 1.0 ns. We found that adding the Δs values, $\Delta s_{12} = \Delta s_1 + \Delta s_2$, and selecting signal events with *either* large $E\!\!\!/_T$ *or* large Δs_{12}, either of which is not SM-like, maximizes the separation of signal and background as shown in Fig. 8. The position of the cuts are optimized for each mass and lifetime to minimize the 95% C.L. cross section limit, and we find that both the Δs_{12} and $E\!\!\!/_T$ cuts are stable at around 7 ns and 50 GeV for non-zero lifetimes. Without timing information we found the optimal $E\!\!\!/_T$ cut to also be around 50 GeV.

2. $\gamma + E\!\!\!/_T + 0$ jets

From efficiency considerations and since the signal does not produce jets at the parton level we expect a $\gamma + E\!\!\!/_T + 0$ jets analysis to yield the best sensitivity for longer neutralino lifetimes. We follow the analysis in [10] (summarized in Table III) and require the highest E_T photon to have $E_T > 25$ GeV and $|\eta| \leq 1$, a minimum $E\!\!\!/_T$ of 25 GeV, and no jets or additional photons with $E_T > 15$ GeV, and study

Table II: The background and baseline selection criteria used for the $\gamma\gamma + E\!\!\!/_T$ analysis following Ref. [3, 21].

Baseline selection requirements:		
$E_T^{\gamma_1} > 12$ GeV, $E_T^{\gamma_2} > 12$ GeV		
$|\eta^{\gamma_1}| < 1$, $|\eta^{\gamma_2}| < 1$		
Backgrounds:		
2,577 events / 100 pb^{-1} from QCD		
$\Delta s_{12} = \Delta s^{\gamma_1} + \Delta s^{\gamma_2}$, $\overline{\Delta s_{12}} = 0$ ns with resolution $\sigma_{\Delta s_{12}} = 1.41$ ns		
$E\!\!\!/_T$: Rayleigh distribution (Square-root of the sum of 2 Gaussians squared) with $\sigma = 10$ GeV		
Optimization:		
Accept events where the event has a $E\!\!\!/_T$ greater than the optimized $E\!\!\!/_T$ cut *or* whose photon has a Δs_{12} greater than the optimized Δs_{12} cut.		

the final selection requirements on $E\!\!\!/_T$ and Δs. The background for this analysis is dominantly QCD, $Z\gamma$ and cosmic ray sources. Since photons from cosmic ray sources hit the detector with no correlation between the arrival time and the time of collision, we expect them to be randomly distributed over time and model this with a flat random distribution in Δs. As in the previous section the Δs of all other SM sources is dominated by the timing resolution of 1.0 ns. The $E\!\!\!/_T$ for the backgrounds are modeled according to the shapes in [10], and extrapolated to large values using an exponential fit. The expected background and signal shapes are shown in Fig. 9. The final cuts on $E\!\!\!/_T$ and Δs are applied to sort out events with a large $E\!\!\!/_T$ *and* whose photon has a Δs within a lower bound and an upper bound: $\Delta s_1 \leq \Delta s \leq \Delta s_2$, to reject photons from SM background as well as from cosmic ray sources. We find the optimized cuts at around $\Delta s_1 = -2.0$ ns, $\Delta s_2 = 2.0$ ns and $E\!\!\!/_T = 80$ GeV. However, Δs_2 could vary up to 3 ns for high lifetimes, $E\!\!\!/_T$ up to 120 GeV for higher masses. Without timing information we found the optimal $E\!\!\!/_T$ cut mostly at around 100 GeV.

3.   Results

Figures 10 and 11 show the expected 95% C.L. cross section upper limits vs. $\tau_{\tilde{\chi}}$ for $m_{\tilde{\chi}} = 70$ GeV/c^2 and vs. $m_{\tilde{\chi}}$ for $\tau_{\tilde{\chi}} = 20$ ns for both analyses for a luminosity of 2 fb^{-1}. Figure 12 shows the ratio of the lower of the two 95% C.L. cross section limits with EM Timing system usage and without in two dimensions. In these plots we see four trends: 1) As a function of lifetime the cross section limits rise since the probability that the neutralinos decay in the detector goes down, 2) at high lifetimes the timing handle is better able to separate the signal from the backgrounds and produces better limits relative to kinematics alone, 3) as a function of mass the cross section decreases as more and more events pass the kinematic threshold, and 4) at low masses the timing handle is better able to separate the signal from the backgrounds because the momentum distribution happens be lower on average (see Fig. 8c which shows an example where the kinematics are such that there is only small additional acceptance from
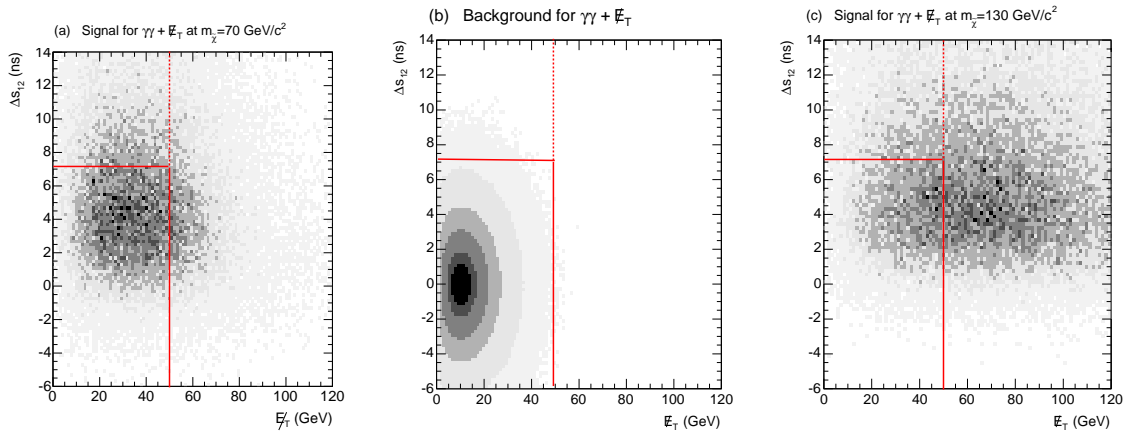
Figure 8: The distribution of Δs_{12} and $\not{E}_T$ for signal and background in the $\gamma\gamma + \not{E}_T$ analysis. The distributions are (a) from direct neutralino pair production, with $m_{\tilde{\chi}} = 70$ GeV/c^2 and $\tau_{\tilde{\chi}} = 10$ ns, (b) QCD background and (c) direct neutralino pair production, with $m_{\tilde{\chi}} = 130$ GeV/c^2 and $\tau_{\tilde{\chi}} = 10$ ns. The solid and dashed lines show the cuts with and without EMTiming system usage respectively that give the smallest 95% C.L. cross section limit. In (c) the mass is so large that there is only small additional acceptance from allowing large Δs_{12} events which is why the sensitivity is not improved in this mass region (see 10).

Table III: The background and baseline selection criteria for the $\gamma + \not{E}_T + 0$ jets analysis following Ref. [10].

Baseline selection requirements:
$E_T^\gamma > 25$ GeV
$|\eta^\gamma| < 1.0$
$\not{E}_T > 25$ GeV
No jets or additional photons with $E_T^{jet} > 15$ GeV
Backgrounds:
12.6 events / 100 pb^{-1} from $Z\gamma \to \nu\bar{\nu}\gamma$, $W\gamma$, $W \to e\nu$, QCD and cosmics
Non-cosmics: $\Delta s = 0$, $\overline{\Delta s_{12}} = 0$ ns with resolution $\sigma_{\Delta s} = 1.0$ ns
Cosmics: 57.2% of total background, flat distribution in Δs $\not{E}_T$ distribution according to [10], and extrapolated using an exponential
Optimization:
Accept events where the event has a $\not{E}_T$ greater than the optimized cut $\not{E}_T$ *and* whose photon has a Δs within a range of optimized cuts $\Delta s_1 \leq \Delta s \leq \Delta s_2$.

allowing large Δs_{12} events). As expected the $\gamma\gamma + \not{E}_T$ analysis yields lower cross sections when the mass or the lifetime is low (see Fig. 12). The ratio is greatest in this region and occurs at a mass around 50 GeV/c^2 and a lifetime of 10-20 ns. The $\gamma + \not{E}_T + 0$ jets analysis yields lower cross section limits for the rest of the considered lifetime range and masses, but it is important to note that the course of the separation line of the analyses depends on the production momentum distribution of the neutralino. Unfortunately this analysis cannot be applied to searches for long-lived NLSP neutralinos in a true GMSB model with the preferred production processes as there the neutralinos are produced as part of cascades from gaugino pairs which contain jets. Therefore, we do a separate

analysis for a full GMSB production in the next section.

IV. SENSITIVITY TO GMSB MODELS

We next consider the sensitivity to full GMSB production where we allow all processes to contribute to the final state according to their predicted cross sections. We use the same simulation tools as in Section III A, with the GMSB parameters chosen according to the Snowmass Slope guidelines [15] in the range where the neutralino is the NLSP. Again we consider a single photon and a diphoton analysis. The $\gamma\gamma + \not{E}_T$ analysis methodology is identical to the case of neutralino pair production, but the single photon analysis must be modified to allow jets as here the neutralinos are part of cascades from gauginos which produce additional particles which, in general, could be identified jets. We thus use a $\gamma + \not{E}_T + $ jets analysis.

A. $\gamma + \not{E}_T + $ jets

A $\gamma + \not{E}_T + $ jets analysis should be most sensitive to neutralinos with long lifetime which are produced in association with other particles in the final state such as from gaugino pair production. We follow the analysis in [11] (summarized in Table IV) and require events with the primary (highest E_T) photon to have $E_T > 25$ GeV and $|\eta| = [0, 1.1]$ or [1.5, 2.0], $\not{E}_T > 25$ GeV, ≥ 2 jets of $E_T > 20$ GeV and $|\eta| < 2.0$, and study the final selection requirements on $\not{E}_T$ and Δs. The backgrounds are dominated by QCD and W+jets [22]. The expected $\not{E}_T$ of the background is modeled according to Ref. [11], and since the backgrounds are from SM we take a mean $\Delta s = 0$ ns with a resolution of 1.0 ns. The signal and background shapes are shown in Fig. 13. We find that the optimal final selection requirements accept events in which the event has a large $\not{E}_T$ or a large Δs. Again, both cuts are optimized to minimize the 95% C.L. cross section limit for each mass and lifetime case. For without-timing usage we find the
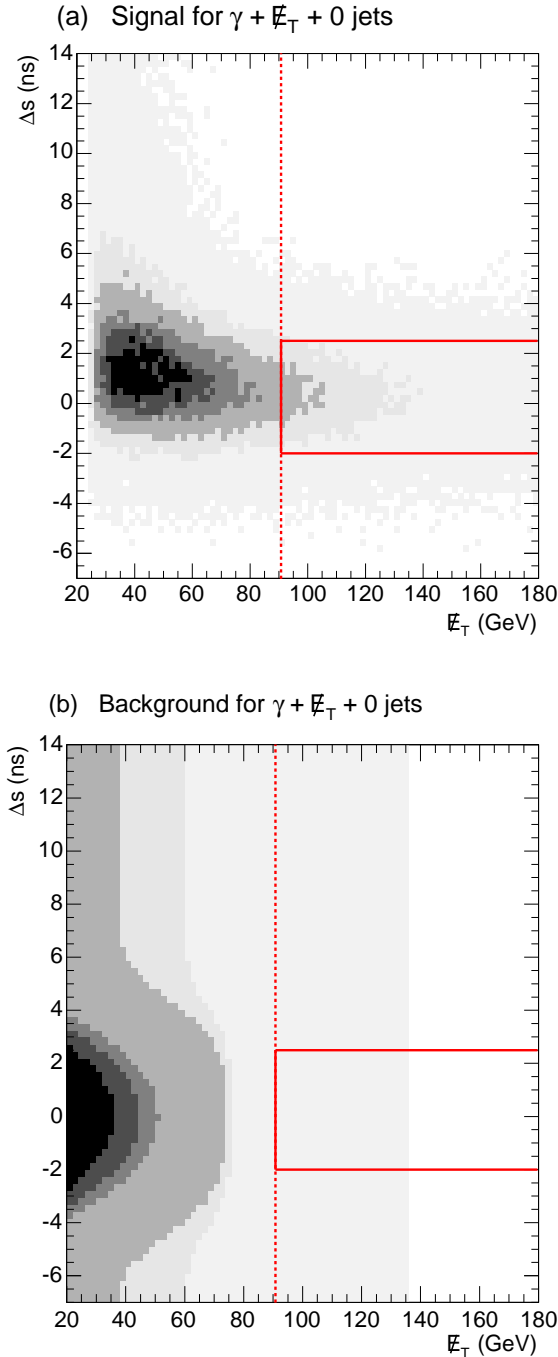
(a)   Signal for $\gamma + \not{E}_T + 0$ jets

Direct $\tilde{\chi}_1^0$-pair production

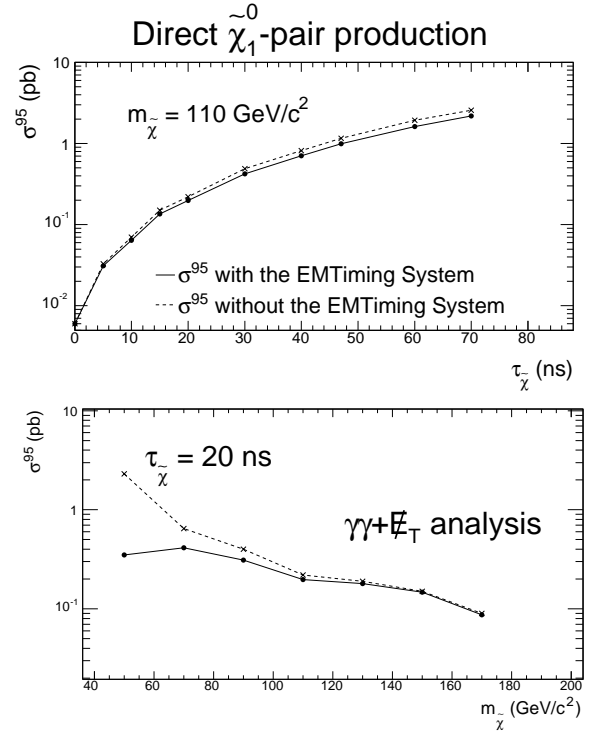(b)   Background for $\gamma + \not{E}_T + 0$ jets

Figure 10: The expected 95% C.L. cross sections limits on neutralino pair production as a function of $\tau_{\tilde{\chi}}$ for $m_{\tilde{\chi}} = 70$ GeV/c^2 (top) and as a function of $m_{\tilde{\chi}}$ for $\tau_{\tilde{\chi}} = 20$ ns (bottom) in the $\gamma\gamma + \not{E}_T$ analysis for 2 fb^{-1} luminosity both with and without a timing system for comparison. As expected at $\tau_{\tilde{\chi}} = 0$ ns the cross sections merge as the timing system has no effect; for higher $\tau_{\tilde{\chi}}$ the sensitivity goes down as more photons leave the detector, but the difference of the limits increases as Δs gets larger for the signal and timing becomes more helpful. The limits get better as the mass goes up since more of the events pass the kinematic requirements, however the timing system only provides real additional sensitivity at the lowest masses where the neutralino momentum distribution is softer.

$\not{E}_T$ cut to be around 50 GeV for masses around 70 GeV/c^2, varying up to 110 GeV for masses around 150 GeV/c^2. For with-timing usage we find only a Δs cut around 4 ns which is stable for all masses and lifetimes, and no $\not{E}_T$ cut other than the baseline $\not{E}_T > 25$ GeV (except for $\tau_{\tilde{\chi}} = 0$ ns where the diphoton case has the best sensitivity). While it is outside of our ability to predict, one might find further optimization is possible by further lowering the baseline selection requirements.

Figure 9: The distribution of Δs and $\not{E}_T$ for signal and background in the $\gamma + \not{E}_T + 0$ jets analysis. The distributions are (a) from direct neutralino pair production, with $m_{\tilde{\chi}} = 70$ GeV/c^2 and $\tau_{\tilde{\chi}} = 10$ ns, and (b) from SM background. The solid and dashed lines show the cuts with and without EMTiming system usage respectively that give the smallest 95% C.L. cross section limit.

B.   Results

Figures 14 and 15 show the expected 95% C.L. cross section upper limits vs. $\tau_{\tilde{\chi}}$ for $m_{\tilde{\chi}} = 70$ GeV/c^2 and vs. $m_{\tilde{\chi}}$ for $\tau_{\tilde{\chi}} = 20$ ns for both analyses for a luminosity of 2 fb^{-1}. Figure 16 shows the ratio of the lowest 95% C.L. cross section limits with EMTiming system usage and without in two
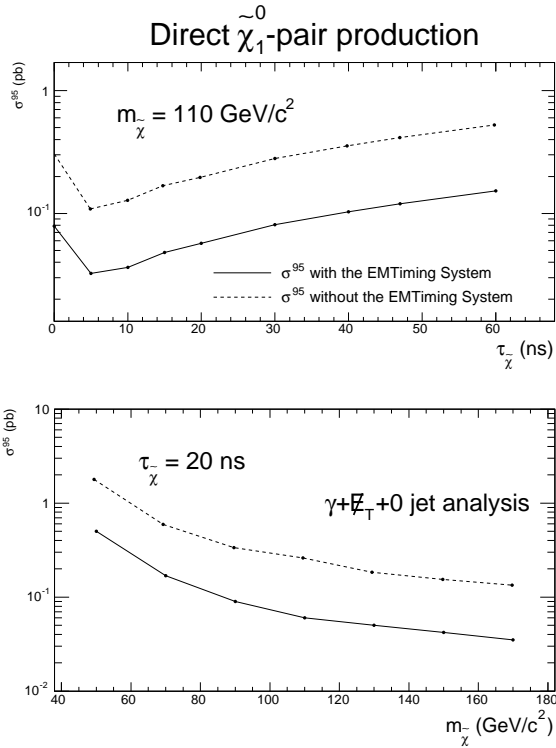
Figure 11: The expected 95% C.L. cross section limits on neutralino pair production as a function of $\tau_{\tilde{\chi}}$ for $m_{\tilde{\chi}} = 70$ GeV/c^2 (top) and as a function of $m_{\tilde{\chi}}$ for $\tau_{\tilde{\chi}} = 20$ ns (bottom) in the $\gamma + \not{E}_T + 0$ jets analysis for 2 fb^{-1} both with and without a timing system. As in Fig. 10, for higher $\tau_{\tilde{\chi}}$ the sensitivity goes down as more photons leave the detector, but the difference of the limits increases as Δs gets larger for the signal and timing becomes more helpful. The curves do not merge at 0 ns lifetime since cosmic ray backgrounds always contribute at high Δs and the timing system always has some effect on the cross section limit. The rise from 10 ns to 0 ns originates in an increasing probability towards zero lifetime for two photons to remain in the detector, yielding lower efficiency for a single photon analysis. The limits get better as the mass goes up since more of the events pass the kinematic requirements.

dimensions. We see the same general trends as in neutralino pair production as the signal shapes are similar in both analyses.

A comparison of the cross section limits with the production cross sections in the GMSB model at a luminosity of 2 fb^{-1} gives the mass vs. lifetime exclusion regions shown in Fig. 17. As expected, timing has the biggest effect at low masses and high lifetimes. We have also indicated the exclusion regions from LEP II from both direct and indirect searches [13], and the line $m_{\tilde{G}} = 1$ keV/c^2, below which is the theoretically preferred region from cosmological constraints [14]. LEP effectively excludes all neutralino masses under 80 GeV/c^2 up to high lifetimes, with a small extension to 100 GeV/c^2 for lifetimes below 20 ns. For 2 fb^{-1}, in run II, the Tevatron should significantly extend the sensitivity at large mass and lifetimes, covering most of the lifetimes for $m_{\tilde{G}} < 1$ keV/c^2 up to a mass of around 150 GeV/c^2. The
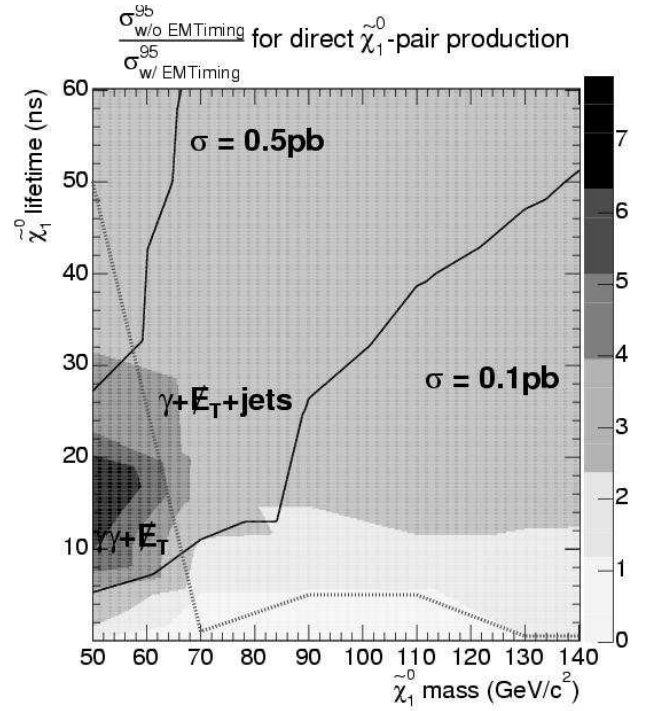

Figure 12: This plot combines the $\gamma\gamma + \not{E}_T$ and $\gamma + \not{E}_T + 0$ jets analysis results for neutralino pair production for 2 fb^{-1} of data and is a 2-dimensional visualization of Figs. 10 and 11. The contours of constant cross section limit are shown as the solid lines, and the separation line between the regions where the two different analyses provide the best sensitivity is given by the dotted line; the $\gamma + \not{E}_T + 0$ jets analysis shows better cross section limits than a $\gamma\gamma + \not{E}_T$ analysis in the mass and lifetime range above the dashed line. The shaded regions delineate the contours of the ratio of the 95% C.L. cross section limits between with and without EM-Timing information. The ratio is greatest for a low neutralino mass and a lifetime of 10-20 ns, and lowest for a high mass and low lifetime.

Table IV: The background and baseline selection criteria used for the $\gamma + \not{E}_T +$ jets analysis following Refs. [11, 22].

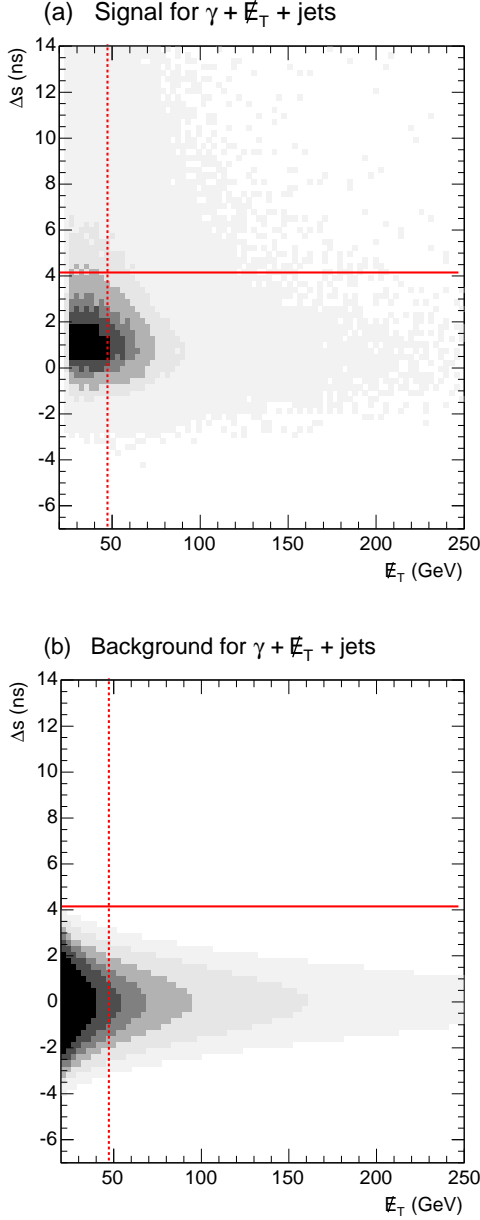| Baseline selection requirements: |
| --- |
| $E_T^\gamma > 20$ GeV |
| $|\eta^\gamma| < 1.1$ and $1.5 < |\eta^\gamma| < 2.0$ |
| $\not{E}_T > 25$ GeV |
| ≥ 2 jets with $E_T^{jet} > 20$ GeV and $|\eta^{jet}| < 2.0$ |
| Backgrounds: |
| 320 events / 100 pb^{-1} from QCD and W+jets |
| $\Delta s_{12} = 0$ ns with resolution $\sigma_{\Delta s} = 1.0$ ns |
| $\not{E}_T$ distribution from [11], extrapolated to large $\not{E}_T$ |
| Optimization: |
| Accept events where the event has a $\not{E}_T$ greater than the optimized $\not{E}_T$ cut *or* whose photon has a Δs greater than the optimized Δs cut. |

(a) Signal for $\gamma + \not{E}_T + $ jets

full GMSB production
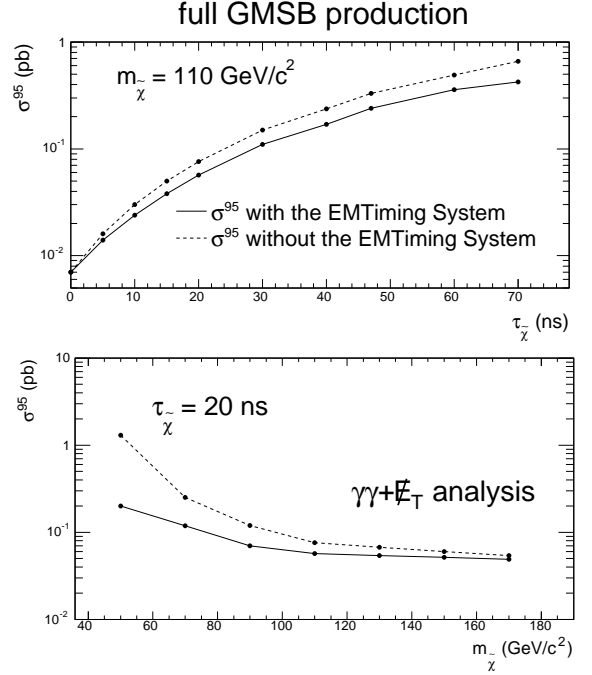

(b) Background for $\gamma + \not{E}_T + $ jets

Figure 14: The expected 95% C.L. cross section limits as a function of $\tau_{\tilde{\chi}}$ for $m_{\tilde{\chi}} = 70$ GeV/c^2 (top) and as a function of $m_{\tilde{\chi}}$ for $\tau_{\tilde{\chi}} = 20$ ns (bottom) at 2 fb^{-1} for with and without EMTiming for full GMSB production in a $\gamma\gamma + \not{E}_T$ analysis. The results are similar to those in Fig. 10.

C. Factors that might change the cross section limit

While we have taken the best available nominal values from the references for both the contamination of cosmic ray background events and the timing resolution in the $\gamma\gamma + \not{E}_T$ and a $\gamma + \not{E}_T + $ jets analyses, the limits are sensitive to mis-estimations of these values. For simplicity, rather than include them as a systematic error we estimate the variation of our results for these effects on our cross section limits for a neutralino mass of 110 GeV/c^2 and a lifetime of 40 ns beyond the LEP II exclusion region. Figure 18 shows the cross section limit as a function of the fraction of events which are from cosmics in the background sample. Using the same analysis style as in the $\gamma + \not{E}_T + 0$ jets case we find cuts around $\Delta s_1 = 3.0$ ns and $\not{E}_T = 55$ GeV, with Δs_2 varying from infinity down to 7 ns with a rising fraction of cosmics. The limits rise approximately linearly as a function of the fraction of events which are from cosmics. An upper bound on the fraction of cosmics of 10% would reduce the limits by about a factor of four; a more reasonable estimate is probably 1-5% which would raise the limts by a factor of 2-3. The limits are potentially more sensitive to the resolution. Figure 19 shows how the limits change as a function of the system resolution for the same mass and lifetime, for the original $\gamma + \not{E}_T + $ jets analysis. While there is a mass/lifetime dependent resolution threshold from where the limit can change drastically and approach the cross section without EMTiming, the limits are fairly stable (with the same factor of 2) for resolutions within
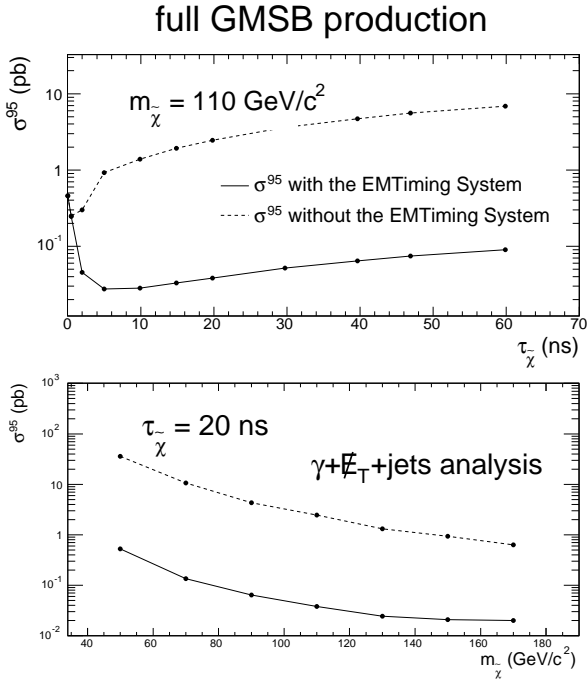
Figure 13: The distribution of Δs and $\not{E}_T$ for signal and background in the $\gamma + \not{E}_T + $ jets analysis. The distributions are (a) from full GMSB production, with $m_{\tilde{\chi}} = 70$ GeV/c^2 and $\tau_{\tilde{\chi}} = 10$ ns, and (b) from SM background. The solid and dashed lines show the cuts with and without EMTiming system usage respectively that give the smallest 95% C.L. cross section limit.

mass exclusion limit at 168 GeV for $\tau_{\tilde{\chi}} = 0$ ns is comparable to the limit presented in the DØ study of displaced photons in Ref. [23], but for large lifetimes this result significantly extends the reach.

full GMSB production

Figure 15: The expected 95% C.L. cross section limits as a function of $\tau_{\tilde{\chi}}$ for $m_{\tilde{\chi}} = 70$ GeV/c^2 (top) and as a function of $m_{\tilde{\chi}}$ for $\tau_{\tilde{\chi}} = 20$ ns (bottom) at 2 fb^{-1} for with and without EMTiming System for full GMSB production in a $\gamma + \not{E}_T +$ jets analysis. For all but the lowest lifetimes the timing information significantly improves the cross section limits. Note that here the cross sections merge at zero lifetime since we have neglected cosmics in this analysis following [11, 22].

20% of the nominal 1 ns resolution, and there is good reason to believe that the resolution will be better than advertised [7].

V. CONCLUSION

We have studied the prospects of using the new EMTiming system at CDF in the search for neutral, long-lived particles which decay to photons, as one can find in supersymmetric models. We find that the kinematic requirements and the EMTiming system provide excellent rejection against SM backgrounds in complementary fashion. As the mass increases the kinematics are more important and the sensitivity gets better. For a given mass, as the lifetime increases more and more of the neutralinos leave the detector and the overall sensitivity goes down, but the EMTiming system provides additional rejection power and allows for significant exclusions even at large lifetimes. While the region where EMTiming produces the most additional rejection is already excluded by LEP II, the additional handle it provides should allow the Tevatron in run II to produce the world's most stringent limit at masses above 80 GeV/c^2 at high lifetimes and has the potential to cover the entire region for $m_{\tilde{G}} < 1$ keV/c^2 up to a neutralino mass of around 150 GeV/c^2.
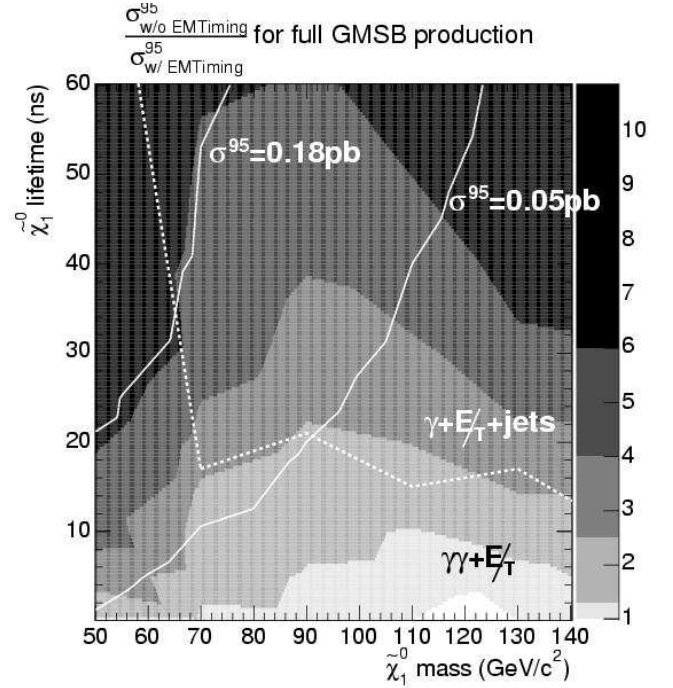

Figure 16: This plot combines the $\gamma\gamma + \not{E}_T$ and $\gamma + \not{E}_T +$ jets analysis results for a full GMSB model simulation for 2 fb^{-1} of data and is a 2-dimensional visualization of Figs. 14 and 15. The contours of constant cross section limit are shown as the solid lines, and the separation line between the regions where the two different analyses provide the best sensitivity is given by the dotted line; the $\gamma + \not{E}_T +$ jets analysis shows better cross section limits than a $\gamma\gamma + \not{E}_T$ analysis in the mass and lifetime range above the dashed line. The shaded regions delineate the contours of constant ratio of the 95% C.L.- cross-section limits between with and without EMTiming information. The EMTiming system has its most effective region at high lifetime and is least effective for high masses, where the kinematics give the best separation.

Appendix A: PHOTON POINTING

As shown in Fig. 17, LEP II has already excluded the low neutralino mass region using a photon pointing method [13].
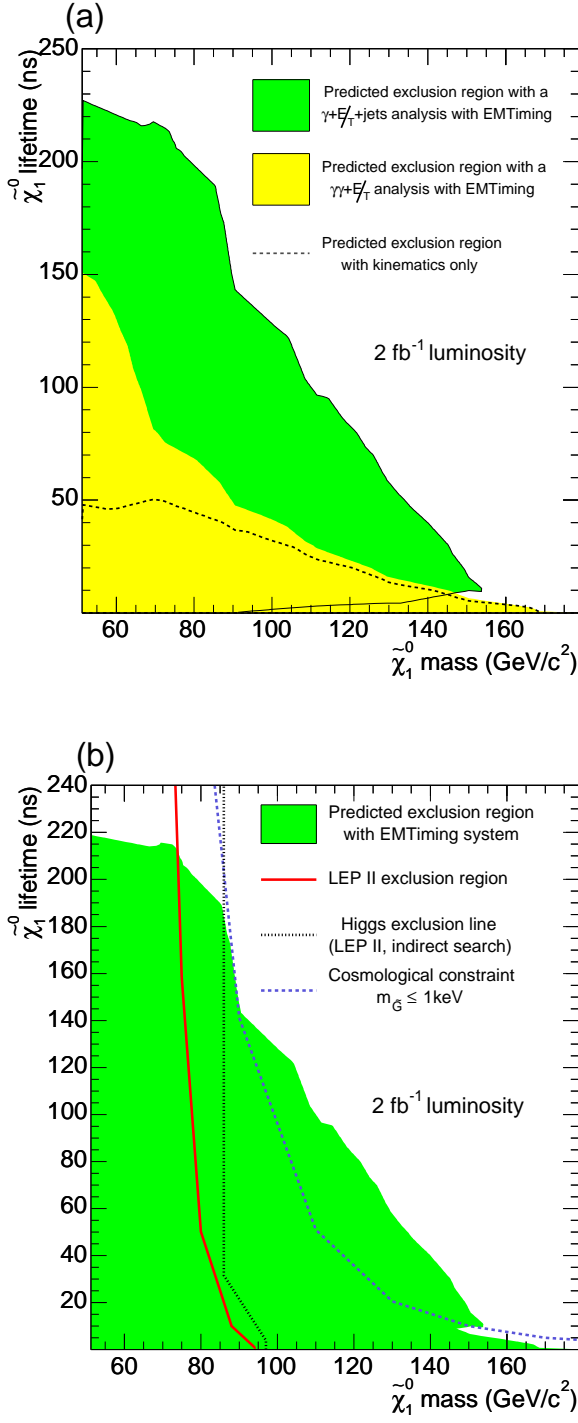
(a)

(b)

Figure 17: The expected 95% C.L. exclusion regions as a function of neutralino lifetime and mass for full GMSB production at 2 fb^{-1} luminosity for the the $\gamma\gamma + \not{E}_T$ and a $\gamma + \not{E}_T +$ jets analysis separately. In plot (a) the region below the dashed line is the exclusion region from kinematics alone, i.e., where no timing information is used. Plot (b) shows the full exclusion region from the overlap of the two analyses and compares the results to the direct and indirect search limits from LEP II [13] and the theoretically favored region from cosmological constraints ($m_{\tilde{G}} < 1$ keV/c^2) [14]. The Tevatron in run II should be able to significantly extend the LEP II limits and provide sensitivity in the favored region for all masses below about 150 GeV/c^2.

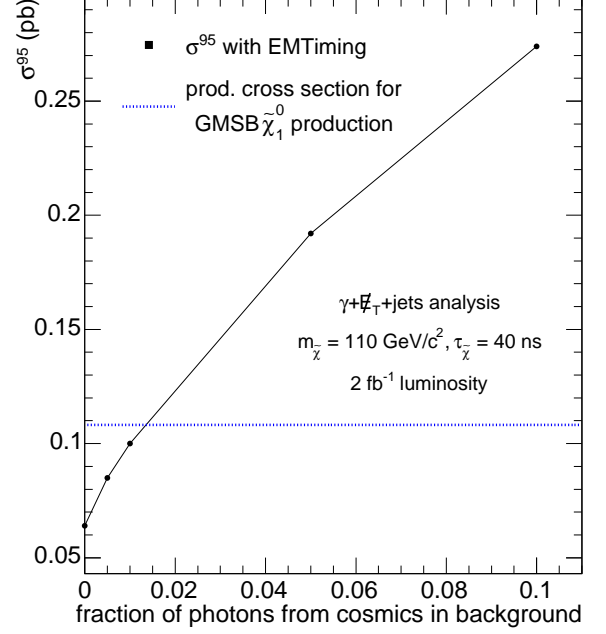Figure 18: The 95% C.L. cross section limit on full GMSB production at $m_{\tilde{\chi}} = 110$ GeV/c^2 and $\tau_{\tilde{\chi}} = 40$ ns as a function of the fraction of the background from cosmic ray sources for a $\gamma + \not{E}_T +$ jets analysis. The cross section limits rise approximately linearly as a function of the fraction and 10% provides an outer bound on this fraction. A more reasonable fraction is probably 1-5% which roughly doubles the limit.

In this section we compare the EMTiming system to a potential photon pointing ability at CDF. A non-zero lifetime can result in a macroscopic decay length and impact parameter, where the impact parameter of the photon is basically the closest distance of the trajectory to the collision point. While CDF has never used its calorimeter for a pointing measurement it is possible to use the central EM strip/wire gas chamber (CES) and the central pre-radiator gas chamber (CPR) at CDF to measure two points along the photon trajectories that determine the direction of the photon, and trace it back to yield the impact parameter [24]. Since the CPR has no z-measurement ability this allows only a measurement of the radial component of the impact parameter with an estimated resolution of 10 cm (see Table V). One of the primary reasons this has not been used is the conversion, i.e. measurement, probability, of $\sim$65%, with an angular dependence obtained with:

$$P_C = 1 - e^{-\frac{N_{\text{rad}}}{\sin\theta}} ,$$

where $N_{\text{rad}} = 1.072$ is the number of radiation lengths before the CPR and θ is the angle with respect to the beamline. To estimate the sensitivity with a pointing method we consider a $\gamma + \not{E}_T +$ jets analysis. Figure 20 shows the distribution of the signal events vs. impact parameter and Δs in a $\gamma + \not{E}_T +$ jets analysis taking into account the measurement probability; there are roughly as many events in the region of low impact parameter and high Δs as there are at high impact parameter and low Δs. Hence either method should have
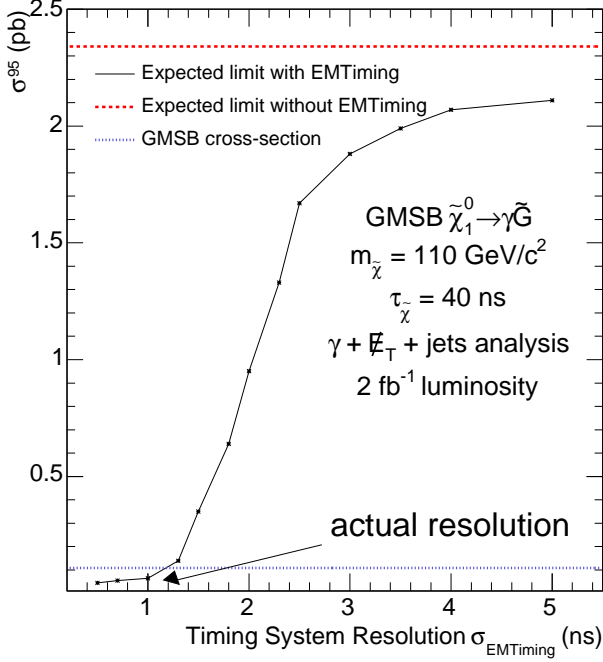
Figure 19: The 95% C.L. cross section limits vs. EMTiming system resolution for $m_{\tilde{\chi}} = 110$ GeV/c^2 and $\tau_{\tilde{\chi}} = 40$ ns at 2 fb^{-1} luminosity in the $\gamma + \not{E}_T +$ jets analysis. As expected, for large resolution the cross section with EMTiming approaches the cross section without EMTiming. A system resolution of 1.0 ns improves the cross section limit by a factor of about 20, but this varies as a function of mass, lifetime and depends on the analysis. It is reasonable to assume that the resolution will be within 20% of the nominal 1.0 ns presented here.

Table V: Photon pointing parameters for the CDF detector [24]. With this combination we estimate an impact parameter resolution of 10 cm in the radial direction.

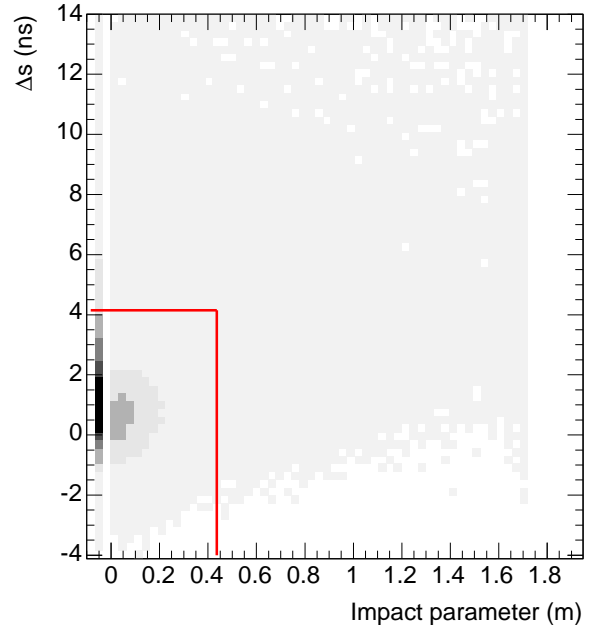| measurement only in radial direction	
Radius of CES	184.15 cm
Radius of CPR	168.29 cm
σ_{CES}	2 mm
σ_{CPR}	5 mm
N_{rad}	1.072 X_0

Figure 20: The relationship between Δs and the impact parameter b of a photon from $\tilde{\chi}_1^0 \to \gamma\tilde{G}$ decays in a GMSB model with $m_{\tilde{\chi}} = 70$ GeV/c^2 and $\tau_{\tilde{\chi}} = 10$ ns. We show the selection requirements that give us the smallest 95% C.L. cross section limit in a $\gamma + \not{E}_T +$ jets analysis. The photons without impact parameter measurement are assigned a $b = -0.1$ m. Due to the low cut on the impact parameter there are about as many events in the low-Δs high-b as in the high-Δs low-b quarter, leading to a similar efficiency for a pure b-cut compared to a pure Δs cut. The combined restriction leads to improved signal sensitivity.

roughly the same effect on the exclusion region, as confirmed by Fig. 21, which shows the expected exclusion region in the mass-lifetime plane. While timing is better than pointing by itself, if pointing turns out to be feasible, a combination of the two would improve the sensitivity.

Considered separately, a second advantage of timing is that it "filters" manifestly long lifetime events, whereas the impact parameter allows also short lifetime-high momentum events, which might come from SM. Another possible advantage of the combination is that in the event of an excess, we could draw more information about the individual events, for instance determine the direction of the photon. With the x-y-direction being fixed by the CPR/CES measurement, we can use the timing system to measure the z-direction. Or if the pointing provided the photon direction in z and x-y, one could possibly determine the position of the vertex and thus the decay time. However, with the current 1.0 ns resolution the photon vertex position resolution would be roughly 50 cm, if we assume the neutralino boost to be ~ 1.0.
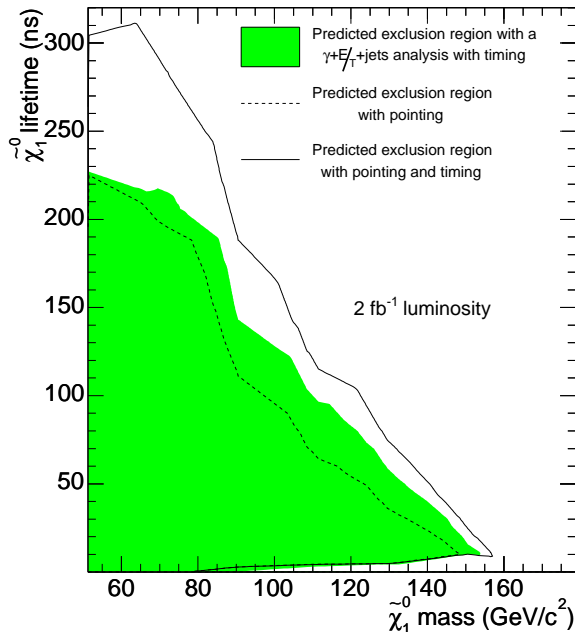
Figure 21: A comparison of the expected exclusion regions as a function of neutralino mass and lifetime for the GMSB model at 2 fb^{-1} luminosity for a $\gamma + \not{E}_T +$ jets analysis with photon pointing and timing. While timing generally yields a higher sensitivity than pointing, both methods would, if we combined them, extend the exclusion region further than either of them alone.

[1] CDF II Collaboration, F. Abe *et. al.*, FERMILAB-Pub-96/390-E.

[2] S. Kuhlmann *et. al.*, Nucl. Instrum. Methods Phys. Res. A **518**, 39 (2004); CDF Collaboration, P. T. Lukens, FERMILAB-TM-2198; for more details see http://hepr8.physics.tamu.edu/hep/emtiming/.

[3] See for example CDF Collaboration, F. Abe *et. al.*, Phys. Rev. D **59** 092002 (1999) and Phys. Rev. Lett. **81**, 1791 (1998).

[4] Note that in principle the system can be used in conjunction with the Time of Flight system to search for charged particles as well. This becomes especially interesting for events in which the charged particle decay in flight and no track is reconstructed.

[5] See for example S. Ambrosanio *et. al.*, Phys. Rev. D **54**, 5395 (1996); C. H. Chen and J. F. Gunion, Phys. Rev. D **58**, 075005 (1998).

[6] At CDF x_f is measured by the shower-maximum detector (CES/PES) in the electromagnetic calorimeter and x_i is the collision point, measured by the Silicon Vertex Chamber (SVX). The t_i is calculated by the Central Outer Tracker (COT) and the Time of Flight (TOF) system which use the momentum and the measured time of flight of the charged particles of the underlying event

emerging from the collision point and t_f is the time of arrival of the photon from the EMTiming system.

[7] M. Goncharov, priv. comm.

[8] DØ Collaboration, S. Abachi *et. al.*, Nucl. Instr. Methods Phys. Res. A **338**, 185 (1994).

[9] DØ Collaboration S. Abachi *et. al.* Phys. Rev. Lett. **78**, 2070 (1997), and B. Abbott *et. al.* Phys. Rev. Lett. **80**, 442 (1998).

[10] CDF Collaboration, D. Acosta *et. al.*, Phys. Rev. Lett. **89**, 281801 (2002).

[11] DØ Collaboration, B. Abbott *et. al.*, Phys. Rev. Lett. **82**, 29 (1999).

[12] Note that we do not assume that any analysis without EMTiming at CDF is robust enough to search for long-lived particles since there are no current collider experiments which have results without an additional handle such as photon pointing as done at LEP or DØ. For a discussion of photon pointing see for example ALEPH Collaboration, D. Decamp *et. al.*, Nucl. Instrum. Methods Phys. Res. A **294**, 121 (1998) and D. Cutts and G. Landsberg, arXiv:hep-ph/9904396.

[13] ALEPH Collaboration, A. Heister *et. al.*, Eur. Phys. J. C **25**, 339 (2002); A. Garcia-Bellido, Ph.D. thesis, Royal Holloway University of London, 2002 (unpublished),

arXiv:hep-ex/0212024.

[14] See for example K. Olive, arXiv:hep-ph/9911307 and references therein.

[15] We follow B. C. Allanach *et. al.*, Eur. Phys. J. C**25**, 113 (2002), and take the messenger mass scale $M_\mathrm{M} = 2\Lambda$, $\tan(\beta) = 15$, $\mathrm{sgn}(\mu) = 1$ and the number of messenger fields $N_\mathrm{M} = 1$; c_Grav (gravitino mass factor) and Λ (supersymmetry breaking scale) unrestricted.

[16] T. Sjöstrand, L. Lönnblad and S. Mrenna, arXiv:hep-ph/0108264. We used version 6.158.

[17] F. Paige and S. Protopopescu, BNL Report BNL38034, 1986; F. Paige, S. Protopopescu, H. Baer and X. Tata, hep-ph/0001086. We use version 7.64 to generate the SUSY masses.

[18] J. Conway, http://www.physics.rutgers.edu/jconway/research/software/pgs/pgs.html. We used version 3.21.

[19] Note that we have chosen a neutralino mass of 70 GeV/c^2 as an example, where the boost of the neutralino is lowest, to better illustrate the separation between single and diphoton case. When we present cross section limits we move to a mass of 110 GeV/c^2 where timing provides sensitivity outside the current GMSB exclusion region from LEP II.

[20] E. Boos, A. Vologdin, D. Toback and J. Gaspard, Phys. Rev. D **66**, 013011 (2002).

[21] Following Ref. [3] we have neglected the contribution from cosmic ray backgrounds. The probability of an event with a real photon and a fake photon from a cosmic ray is small, and can be removed with simple topology cuts with very high efficiency. Similar arguments hold for the even more unlikely case of two fake photons from cosmic ray background sources.

[22] Following [11] we have neglected the contribution from cosmic ray backgrounds. The probability of an event with two jets overlapping with a photon from a cosmic ray is small, and and might be removed by requiring events where the photon is equal in magnitude and opposite in ϕ of the $\not{E}_T$.

[23] R. Culbertson *et. al.*, hep-ph/0007080 (especially Fig. 18 therein).

[24] L. Balka *et. al.*, Nucl. Instr. Methods Phys. Res. A **267**, 272 (1988); CDF Collaboration, F. Abe *et. al.*, Phys. Rev. Lett. **73**, 2662 (1994); D. Partos, Ph.D. thesis, Brandeis University, 2001, FERMILAB-THESIS-2001-21.